An analysis of Instantaneous Angular Speed measurement errors

Quentin Leclère[1], François Girardin[1] and Didier Rémond[2]

[1]INSA-Lyon, LVA, F-69621, France
[2]Université de Lyon, CNRS, INSA-Lyon, LaMCoS UMR5259, F-69621, France
{quentin.leclere, francois.girardin, didier.remond}@insa-lyon.fr

Abstract

The instantaneous angular speed (IAS) of a rotating machine is a crucial information to understand the machine operation and to diagnose potential faults. There are several difficulties related to the assessment of the IAS, which is generally estimated using an angle encoder. First of all the IAS is never really instantaneous data, it is always averaged between two increments of the encoder, leading to a spectral aliasing error. The second potential source of estimation error is linked to the manner the time delays between angle increments are measured. A first possibility is to use a high frequency counting approach: a high frequency pulse signal is used as reference, typically several tens of MHz, and an electronic device is used to count the number of pulses of the high frequency clock between two events of the angle encoder signal. A second possibility is to use a standard analog to digital converter with an anti-aliasing filter to acquire the angle encoder signal, using a lower sampling rate (typically several tens of kHz), and to determine event's times of the encoder by numerical processing like upsampling or interpolation. For both approaches, the counting error is related to the uncertainty of the estimated time between two pulses of the angle encoder. A third potential cause of IAS estimation error is related to the angle encoder itself. The encoder is made of a rotating device linked to the shaft, on which a given number of marks are distributed on the whole circumference (the angle between two marks being the resolution of the encoder). These marks can be either teeth or holes, or alterning sectors, depending on the technology (magnetic, optical, ...). In all cases, the angle between consecutive marks is never perfectly the same all around the encoder. These imperfections are the cause of geometrical errors on the estimated IAS.
The aim of this paper is to give some guidelines to handle globally these estimation errors, and to propose a calibration procedure to correct the geometrical error. Some examples will be given on both numerical and experimental illustrations.

1 Introduction

The instantaneous angular speed (IAS) of a rotating machine can be of major interest for real-time monitoring or diagnosis applications. The rotation of the shaft is indeed the result of the global operation of the machine, thus carrying information about all mechanical processes contributing to the rotation. Any fault, failure or defect has theoretically an effect on the instantaneous speed. IAS has widely been used in the monitoring of reciprocating engines [1, 2, 3], gear transmissions [4, 3], rolling bearings [5], or machining [6].

The IAS of rotating machines is generally assessed using a angle encoder, which is basically made of a rotating wheel with marks, and a fixed sensor delivering a signal carrying the mark passing frequency. Several methods can be used to acquire such a signal, either using a high frequency counting approach [7, 8] or post processing the signal acquired with a standard ADC DAQ [9]. The analysis of errors is of course an important issue when dealing with such signals, associated by either measurement noise [10], counting errors [11] or more recently by geometric error [12].

The aim of this paper is to give an overview of potential causes of IAS estimation errors, associated to two different acquisition methods: the high frequency counting approach and the standard DAQ system approach. The first method uses a high frequency counting electronic device, counting the number of elementary periods between two events of the encoder. The second method is based on the use of a standard DAQ to digitalize

the encoder signal, using a sampling frequency much lower than the one used for the counting approach. The time durations between consecutive encoder events are then estimated using interpolation. The first section of the paper is dedicated to errors due to spectral aliasing, induced by the fact the estimated IAS is average over angular periods defined by the encoder resolution. The second part focuses on counting errors, for which a model is established for both methods. In the third section, the causes of geometric error are discussed, and a calibration method is proposed to attenuate it. The last section is devoted to experimental illustrations.

2 Errors due to spectral aliasing

The IAS (Instantaneous Angular Speed) assessed using an angle encoder is never strictly instantaneous data [11]. The speed is estimated from a measure of the time duration between two events of the encoder. The resulting speed is in fact averaged data, over an angle length equal to the encoder resolution $\Delta\theta$. This averaging operation can generate differences between the real IAS and the estimated IAS, because of spectral aliasing. This effect is not easy to formulate because the time duration between two angle steps is not constant. However, the averaging process can be formulated in angle to simplify the analysis:

$$\bar{\omega}(\theta) = \frac{\Delta\theta}{\Delta t} = \Delta\theta \left(\int_{\theta-\Delta\theta/2}^{\theta+\Delta\theta/2} \frac{d\theta}{\omega(\theta)} \right)^{-1} \approx \frac{1}{\Delta\theta} \int_{\theta-\Delta\theta/2}^{\theta+\Delta\theta/2} \omega(\theta) d\theta \tag{1}$$

the approximation in equation (1) being reasonable for small speed fluctuations. The local moving averaging process in angle can be expressed in the Fourier domain using a simple multiplication:

$$\bar{\omega}(\nu) = \omega(\nu)\ \mathrm{sinc}(\pi\nu\Delta\theta) \tag{2}$$

A second intrinsic characteristic of IAS data is that it is sampled at a sampling frequency $1/\Delta\theta$. This angular domain sampling is equivalent to a convolution of the IAS spectrum by a comb filter with a period of $1/\Delta\theta$. This operation generates spectral aliasing if the IAS spectrum is not null above $1/(2\Delta\theta)$ (the Nyquist frequency), which is not guaranteed at all by the low pass filtering expressed in Eq. (1), as illustrated in figure 1.

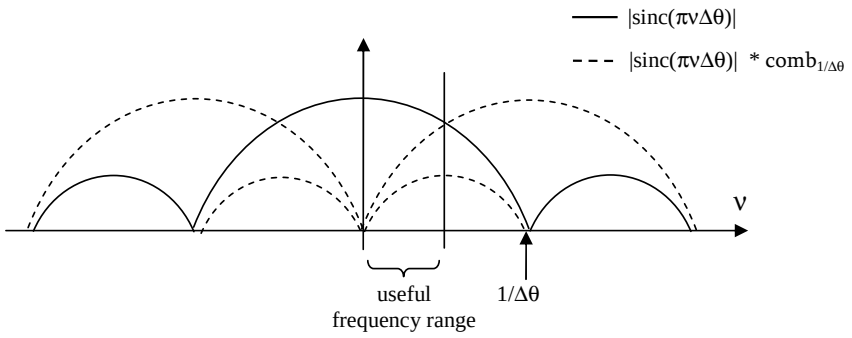

Figure 1: Spectrum of the local averaging operator, and spectrum of the sampled local averaging operator.

2.1 Numerical illustration

A numerical illustration is conducted for the IAS given by the following function:

$$\omega(\theta) = 100 + \mathrm{sign}(\sin(25\ \theta)) \tag{3}$$

The real IAS is simulated with an angular resolution of $d\theta = 2\pi/Z$ radian, with $Z = 1e5$. The corresponding time history is estimated by numerical integration. The measured IAS is simulated for an encoder resolution of $\Delta\theta = 2\pi/N$ radian, $N = 720$ corresponding to the number of pulses by encoder revolution. The angular spectra of the measured and real IAS are given in figure 2, for the useful frequency range of the simulated measured IAS. The energy of the real IAS spectrum is distributed on odd harmonics of order 25, which is characteristic of the square nature of the generated signal. The measured IAS spectrum on odd harmonics of order 25 is slightly underestimated because of the spectral weighting by the cardinal sine (cf. equation 2), and several ghost harmonics are observed between real harmonics because of spectral aliasing.

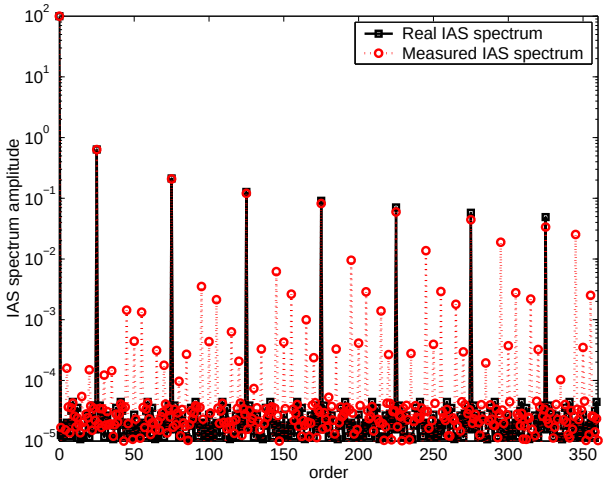

Figure 2: Angular spectra of the real (solid black) and measured (dotted red) IAS. Numerical simulations.

3 Counting error

3.1 High frequency counting approach

The counting error results from the manner the time delays between angle increments are measured. The first possibility is to use a high frequency clock delivering pulses at a high frequency. An electronic device is used to count the number of pulses of the high frequency clock between two angle increments. Of course, this number of pulses is an integer, which generates a rounding error on the estimated time delays, also called quantification error [11].

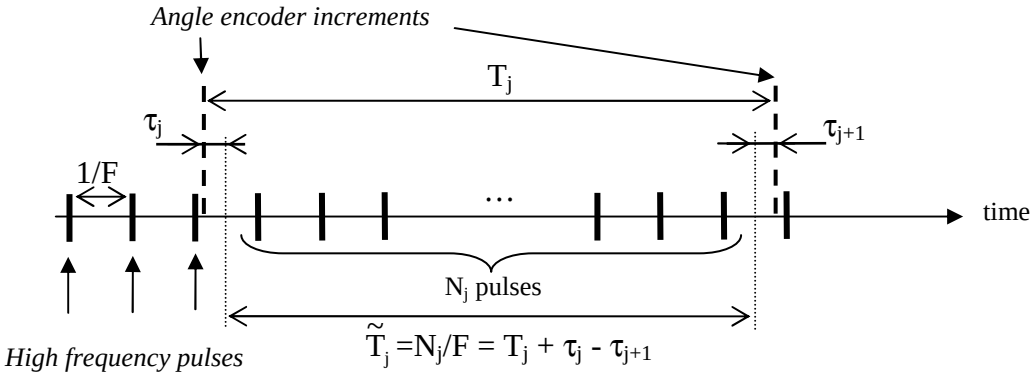

Figure 3: Counting error when using a high frequency pulse counting approach.

The error made on the determination of time occurrences of angle increments is considered here as independent random variables, noted τ_j for increment j, uniformly distributed between $-1/(2F)$ and $1/(2F)$, where F is the frequency of the high frequency clock. Note that tau_j is here defined as the difference between the estimated time occurrence of the encoder increment and the real one (see Fig. 3).

The estimated IAS with counting error is thus expressed as follows:

$$\tilde{\omega}_j = \frac{\Delta\theta}{T_j + \tau_{j+1} - \tau_j} \approx \bar{\omega}_j - \frac{\Delta\theta}{T_j^2}(\tau_{j+1} - \tau_j) \tag{4}$$

The spectrum of the IAS is then given by:

$$\hat{\tilde{\omega}}_k = \hat{\tilde{\omega}}_k - \frac{\Delta\theta}{N}\sum_{j=0}^{N-1}\frac{\tau_{j+1}-\tau_j}{T_j^2}\, e^{-i2\pi jk/N} \tag{5}$$

Let us now assume that the IAS variation effects are negligible, or that the speed is simply constant: $T_j = T = \Delta\theta/\Omega$. After few rearrangements it gives, for $k > 0$:

$$\hat{\tilde{\omega}}_k = \frac{\Omega^2}{N\Delta\theta}\left(\tau_N e^{-i2\pi k(N-1)/N} - \tau_0 + 2i\sin(\pi k/N)e^{i\pi k/N}\sum_{j=1}^{N-1}\left(\tau_j\, e^{-i2\pi jk/N}\right)\right) \tag{6}$$

Of course, the spectrum of the real IAS is in this case equal to zero for $k > 0$, the spectrum given in equation 6 can thus be considered as the contribution of the counting error. It is interesting to give the expected value of the energy of the counting error, as a function of k:

$$E\left[|\hat{\tilde{\omega}}_k|^2\right] = V\left[\hat{\tilde{\omega}}_k\right] = \frac{\Omega^4}{N^2\Delta\theta^2}\left(4(N-1)\sin^2(\pi k/N)+2\right)\, V[\tau], \tag{7}$$

with, remembering that τ is uniformly distributed between $-1/(2F)$ and $1/(2F)$,

$$V[\tau] = \frac{1}{12F^2} \tag{8}$$

3.2 Numerical illustration

We consider the following law of instantaneous speed:

$$\omega(\theta) = \Omega + |\sin(\theta/2)| + \frac{1}{10}\frac{\theta}{2\pi M} \tag{9}$$

where M corresponds to the number of cycles. The first term (Ω) corresponds to a constant component, set successively to 10 rad/s and 100 rad/s. The second term in $|\sin(\theta/2)|$ introduces a periodicity of the speed equal to 2π. The last term introduces a very small acceleration to avoid numerical artifacts encountered when considering a pure constant speed: the speed increases of 0.1 rad/s during the whole simulation, from Ω to $\Omega +$ 0.1 rad/s. $\omega(\theta)$ is computed with a relatively fine resolution of $d\theta = 2\pi/Z$, with $Z = 1e5$. The corresponding time history is obtain by simple numerical integration:

$$t[\theta_p] = \sum_{i=1}^{p}\frac{d\theta}{w[\theta_i]} \tag{10}$$

The angle encoder used in the simulation has $N = 2048$ pulses per revolutions: $\Delta\theta = 2\pi/2048$. The time corresponding to the angle encoder t_j for $j \in [1...NM]$ increments are determined by interpolation of $t[\theta_k]$. The IAS without the counting error (but with aliasing, though negligible for this illustration) is calculated from these data:

$$\bar{\omega}_j = \frac{\Delta\theta}{t_{j+1}-t_j} \tag{11}$$

The counting frequency is adjusted to $F = 80$MHz. The number of events of the high frequency clock that are elapsed between two consecutive encoder increments are then obtained as follows:

$$n_j = \text{floor}(F.t_{j+1}) - \text{floor}(F.t_j) \tag{12}$$

where floor(x) stands for the largest integer less than x. n_j with $j \in [1...NM]$ corresponds typically to the output of a counter connected to an angle encoder. The IAS with counting error is finally:

$$\tilde{\omega}_j = \frac{F\Delta\theta}{n_j} \tag{13}$$

The Discrete Fourier Transform of the IAS with and without counting error is computed at each cycle, for $\Omega = 10$ rad/s and 100 rad/s. The squared modulus of the DFT is then averaged over cycles. The result are

drawn in Fig. 4, together with the expected value of the contribution of the counting error given in equation 7. Note that the only difference between IAS spectra for $\Omega = 10$ rad/s and 100 rad/s is at $k = 0$. It can be seen in Fig. 4 that the contribution of the counting error is largely dominant over a wide high frequency range, and in good agreement qualitatively and quantitatively with the prediction. The amplification of the counting error between $\Omega = 10$ rad/s and 100 rad/s is conform to equation (7): a factor 10 on the average rotation speed induces a factor 100 on the counting error.

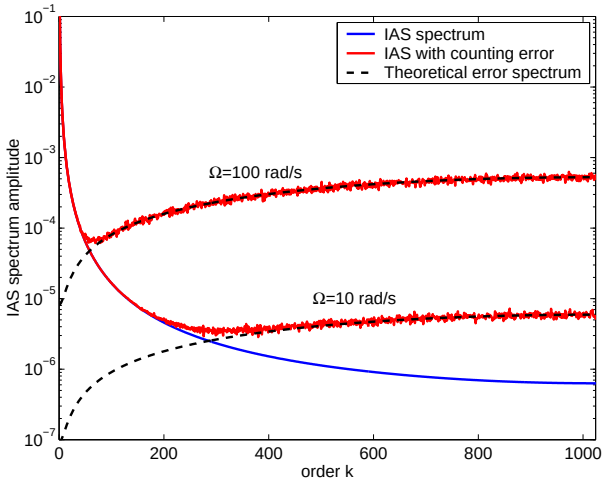

Figure 4: IAS spectrum with and without counting error. Numerical illustration.

3.3 Standard DAQ system approach

Another way to assess the IAS is to post process the signal of the encoder recorded using a standard DAQ system, with a frequency sampling much smaller than the one used in the high frequency counting approach. The idea is to interpolate zero-crossings of the encoder from its low-pass filtered signal. The error made on

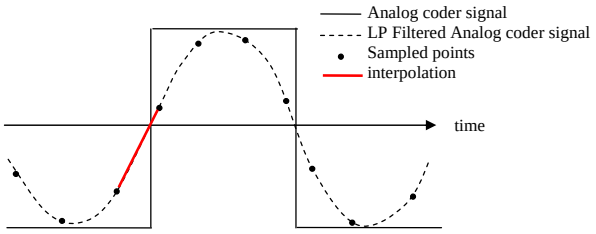

Figure 5: Zero-crossing interpolation using a standard DAQ system.

zero crossing (and thus on the angle increment times) is more difficult to handle than for the high frequency approach. However, the same formalism can be used, just by changing the distribution of τ, the error made on the estimated zero crossing times. The distribution used in the previous section was uniform. For the approach described in this section, a Gaussian centered distribution will be assumed, all the difficulty being to determine its variance.

4 Geometric error

4.1 Effect of the geometric error on the IAS spectrum

A third potential cause of IAS estimation error is related to the angle encoder itself. The encoder is made of a rotating device linked to the shaft, on which a given number of marks are distributed on the whole circumference (the angle between two marks constituting the resolution of the encoder). These marks can be either teeth or

holes, or alterning sectors, depending on the technology (magnetic, optical, ...). In all cases, the angle between consecutive marks is never perfectly the same all around the encoder. These imperfections are the cause of geometrical errors on the estimated IAS. Let us note δ_j the positioning error of the encoder mark j. The effect of the geometric error on the estimated IAS is thus simply as follows:

$$\tilde{\omega}_j = \frac{\Delta\theta}{T_j} = \frac{\Delta\theta_j + \delta_j - \delta_{j+1}}{T_j} = \bar{\omega}_j - \frac{\delta_{j+1} - \delta_j}{T_j} \tag{14}$$

which is quite similar to equation 4, replacing the zero-crossing time error by the geometric error. The spectrum of the estimated IAS with geometric errors is thus:

$$\hat{\tilde{\omega}}_k = \hat{\bar{\omega}}_k - \frac{1}{N}\sum_{j=0}^{N-1} \frac{\delta_{j+1} - \delta_j}{T_j}\, e^{-i2\pi jk/N} \tag{15}$$

Let us now focus on the spectrum of the IAS acquired during one revolution of the encoder. In this case, N corresponds to the number of marks on the encoder's disk. The angular reference can be arbitrarily set to the first mark $j = 0$. In this case, $\delta_0 = \delta_N = 0$. Then, assuming that the speed fluctuation is negligible, the spectrum of the IAS for $k > 0$ is:

$$\hat{\tilde{\omega}}_k = \frac{\Omega}{N\Delta\theta} 2i \sin(\pi k/N) e^{i\pi k/N} \sum_{j=1}^{N-1} \left(\delta_j\, e^{-i2\pi jk/N}\right) \tag{16}$$

The shape of the spectrum of the geometric error is then given as follows:

$$E\left[|\hat{\tilde{\omega}}_k|^2\right] = V\left[\hat{\tilde{\omega}}_k\right] = \frac{\Omega^2}{N^2\Delta\theta^2}\left(4(N-1)\sin^2(\pi k/N)\right)\, V\left[\delta\right] \tag{17}$$

where $V[\delta]$ characterizes the precision of the encoder. It is interesting to note that the shape of the geometric error spectrum is the same than the shape of the counting error spectrum, with a weighting in $\sin^2(\pi k/N)$ for order k.

There is however a major difference between the counting and geometrical errors. The former is a purely random process linked to the measurement uncertainty, while the latter is due to the fact that the exact angle steps of the encoder are not known exactly, and wrongly assumed to be constant. The consequence is that the geometric error, that is repeated cycle to cycle, will exhibit a strong first order cyclostationarity (periodicity), while the counting error will be purely random. In other words, an averaging over cycles of the squared modulus of the IAS will converge to its expected value for the counting error only. A convergence of the geometric error would have been encountered for an averaging over different angle encoders instead of an averaging over cycles.

4.2 Correction of the geometric error

The geometric error can be efficiently reduced by taking into account the real angle steps of the encoder, noted $\Delta\theta_j$. These steps have to be assessed during a calibration procedure. The encoder has to be mounted on a rotating machine operating ideally constant rotation speed: the first order cyclostationarity of the real IAS has to be as small as possible. Then the time intervals T between angle steps have to be acquired during several cycles, in order to average out the counting error by synchronous averaging:

$$\left\langle T_j \right\rangle = \frac{1}{M}\sum_{c=1}^{M} T_{jc} = \frac{1}{F}\left\langle n_j \right\rangle = \frac{1}{FM}\sum_{c=1}^{M} n_{jc} \tag{18}$$

where j stands for the j^{th} angle step, c denotes the c^{th} cycle, M the total number of cycles, and n_{jc} the number of events of the high frequency clock, if the high frequency counting approach is used. Then, assuming that the speed is constant, angle steps can be estimated simply by:

$$\Delta\theta_j = \Delta\theta + \delta_{j+1} - \delta_j = \Omega\left\langle T_j \right\rangle = \frac{2\pi\left\langle T_j \right\rangle}{\sum_{j=1}^{N}\left\langle T_j \right\rangle} = \frac{2\pi\left\langle n_j \right\rangle}{\sum_{j=1}^{N}\left\langle n_j \right\rangle} \tag{19}$$

The main hypothesis when assessing the geometric error with equation (19) is that the speed should be constant. In fact, this condition is not strictly necessary, a less restrictive condition would be that the expected

value of the IAS over cycles at each step of the encoder should be the same, or in other words that the first order cyclostationarity part of the IAS should be constant. This means that all periodic fluctuations of the IAS (at a period equal to 2π or any entire multiple) should be avoided. But unfortunately, this condition is very difficult - not to say impossible - to satisfy: the rotating device is never perfectly balanced, the load is potentially periodic... Anyhow, it is possible to assess the geometric error for different operating conditions (speed, load) of for different encoder/shaft coupling angle, or even for different rotating machines, in order to verify the stability of the result.

5 Experimental illustrations

5.1 Experimental setup

In order to approach the perfect rotating machine, a NC lathe Optimab 350 has been used. A special workpiece is first machined on the lathe, and then encoders are mounted according to Fig. 6. The rotation of the encoder's stator is blocked using a support on a drill, hold on the tool turret. Two optical encoders are studied in this paper, a Heidenhain ERN 120 with a resolution of 2048 pulses/revolution (Fig. 6, center) and an AVL 364 with 720 pulses/revolution (Fig. 6, left). The driving system of Optimab 350 is composed of small pulley

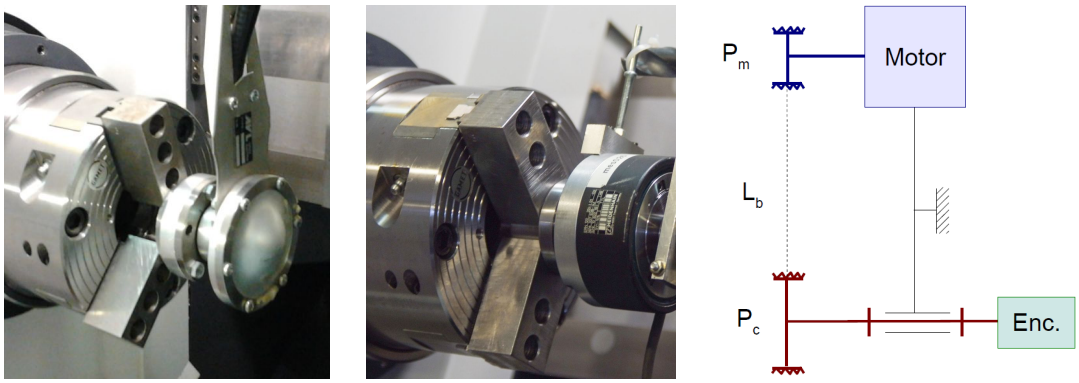

Figure 6: Left : AVL 364 encoder mounted on the chuck. Center : Heidenhain encoder mounted on the chuck. Right : driving mechanism of the lathe.

directly mounted on the motor, linked through a Poly-V belt to a bigger pulley which is part of the chuck shaft. The motor is a three-phase four-pole (pairs) squirrel-cage induction motor (ref. 1PH7107), driven by numerical servo-driver. The speed is thus numerically controlled and is supposed to be - very close to - constant. Angular speed can be driven from 60 rpm to 5000 rpm, in both directions. As ratios between the chuck pulley perimeter Pc and belt length Lb or motor pulley perimeter Pm are not integers (see table 1), the first order cyclostationarity due to rotating system is reduced to coaxiality and run-out precision. Typical coaxiality precision is about 0.05 mm for the assembly [chuck+workpiece]. The IAS measured with the AVL 364 encoder is assessed using

	Chuck pulley	Motor pulley	Belt
Perimeter /length (mm)	625	350	2335
Ratio to Pc	1	1.78	0.27

Table 1: Optimab 350 driving system parameters

the standard DAQ system approach, the angle encoder signal is digitalized with an OROS OR38 system, with a frequency sampling at 102400Hz (24 bits). The IAS measured with the Heidenhain ERN 120 encoder is obtained using the high frequency counting approach, with a NI Compact RIO [9178+9401], with intergrated counter based on 80 MHz high frequency clock. The IAS is estimated at two rotation speeds for the AVL encoder (100 and 500 rpm) and five rotation speeds for the Heidenhain encoder (100, 500, 1000, 2000, 3000).

5.2 Calibration (correction of the geometric error)

The geometric error is assessed for both angle encoders, using equation (19), and for several rotation speeds. The measured angle steps are drawn in Fig. 7, and their empiric standard deviations are given in table 2, for the lowest rotation speed (10.5 rad/s). It can be seen in Fig. 7 that the identified angle steps are very similar for different rotation speeds, which validates the hypothesis discussed in section 4.2. The identified standard deviation of the geometric error is very different for the two encoders, about 20 times lower for the Heidenhain than for the AVL. Another notable fact is that the geometric error signals exhibit strong transient components, reflecting some localized default on the encoder's disks. These defaults, as well as the whole geometric error data, can be seen as a kind of signature of the encoder. It is noteworthy that this signature can be used to get an absolute angle reference, avoiding the necessity to use an additional revolution trigger signal [12, 13]. The

Encoder	N	std($\Delta\theta$)	std($\Delta\theta$)/mean($\Delta\theta$)
AVL 364	720	1.4e-5 rad	0.16 %
Heidenhain ERN 120	2048	7.3e-7 rad	0.024 %

Table 2: Measured standard deviation of the geometric error for the two encoders

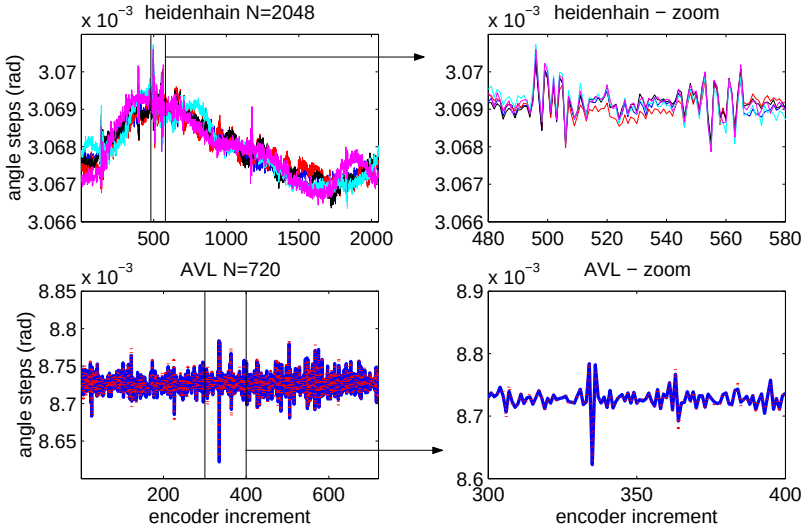

Figure 7: Measured angular steps of the 2 angle encoder and several rotation speeds. Top: Heidenhain encoder, $\Omega = 10.5, 52, 105, 210, 314$ rad/s. Bottom: AVL encoder, $\Omega = 10.5, 52$ rad/s.

IAS spectrum obtained at low speed with both encoders are drawn in Fig. 8, with and without correcting the geometric error. Note that the constant component of the spectrum (at 10.5 rad/s) is largely out of the figure axes, and that the order is limited to $k = 200$ for both encoders, even if their Nyquist orders are different (360 for the AVL and 1024 for the Heidenhain). The two encoders are giving equivalent results up to order 30, and the correction is not significant. Concerning the Heidenhain encoder, the correction is actually not significant on the whole spectrum, due to the very low standard deviation of $\Delta\theta$ (cf table 2). The correction has a substantial effect for the AVL encoder above order 30: the IAS spectrum obtained with correction is significantly lowered, reaching the spectrum obtained using the Heidenhain encoder between orders 30 and 80. Above order 80, the two encoders are giving different results, which could mean that the assembly of the device on the lathe affects the measured IAS.

Some peaks are clearly visible on the IAS spectrum at orders 7, 11, 21 and 43, illustrating clearly that the hypothesis of constant speed is not totally fulfilled. However, these peaks are not suppressed by the correction of the geometric error, which means that they do not contribute to the periodic part of the IAS spectrum. The true orders of the involved phenomena are thus not integers. Remembering that ratios to chuck pulley perimeter is 0.27 for belt and 1.78 for the motor pulley, these two parts are not the cause of speed variations. Nevertheless,

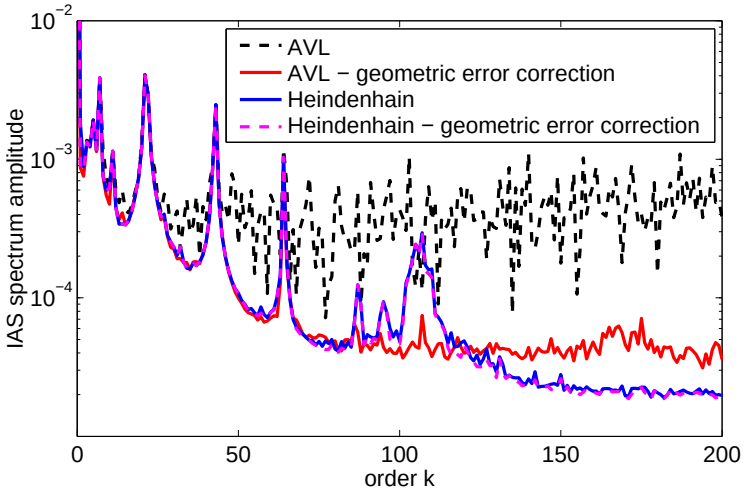

Figure 8: IAS spectrum measured at $\Omega = 10.5$ rad/s using both encoders, with and without the correction of the geometric error.

the motor is a three-phase induction motor, with four pole pairs, that corresponds to 3x4x2=24 windings. Thus, orders 7, 11, 21, 43 corresponds to motor specific orders through belt pulley system (ratio 1.78), that is to say respectively 4 poles, 6, 12, and 24 windings. Orders 6 and 12 are perhaps not linked to stator windings, but the constitution of the rotor is not known. These orders could be due to number of elements in the cage.

5.3 Estimation of the counting error

5.3.1 Using the high frequency counting approach

The IAS spectrum obtained using the Heidenhain encoder, and with the high frequency counting approach, is shown in Fig. 9 (left) for 2 rotation speeds, up to order 1024. Some peaks are oberved at low orders, but the shape of the spectrum at higher orders (above about 300) is conform to the shape of the theoretical counting error spectrum (weighting in $\sin^2(\pi k/N)$ of equation 7). However, the amplitude is largely underestimated. The ratio between theoretical and experimental error spectra is estimated for each rotation speed, and the scaled theoretical counting error spectrum is also drawn in figure 9 (left). The scaling factors are given in table 3. The level of the counting error spectrum is determined by the variance of τ (eq. 7). The theoretical and measured variances of τ are also given in table 3. At low speed (10.5 rad/s), the measured standard deviation of τ is about 7 times higher than the theoretical one, which means that the detection of events of the angle encoders is about 7 times less accurate than expected. This ratio decreases when the speed increases: at 314 rad/s, the measured variance almost equals the theoretical one. This unexpected measurement uncertainty, depending on the rotation speed, is not fully understood for the time being, but the electronic device generating the TTL signal from the physical information of the encoder is strongly suspected.

Rotation speed (rad/s)	theoretical std(τ)= $(12F)^{-1/2}$	experimental std(τ)	scaling ratio
10.5	3.6e-9s	27e-9s	7.4
52	3.6e-9s	9e-9s	2.4
105	3.6e-9s	6e-9s	1.70
210	3.6e-9s	5e-9s	1.26
314	3.6e-9s	4e-9s	1.18

Table 3: Theoretical and measured standard deviation of τ for the high frequency counting method.

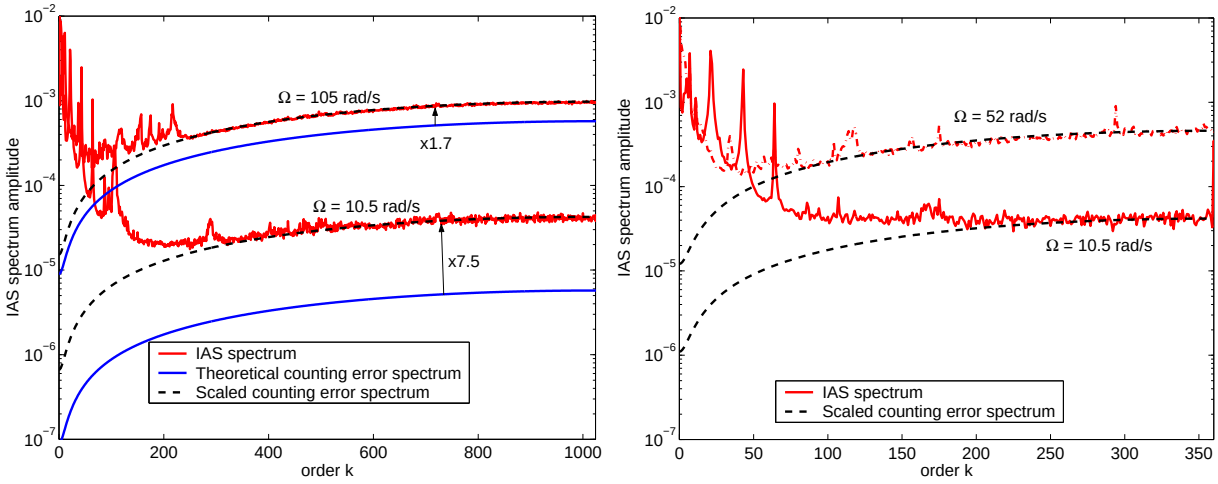

Figure 9: Left: Heidenhain angle encoder (N=2048). IAS spectrum and (scaled) theoretical counting error contribution, using the high frequency counting approach. Right: AVL angle encoder (N=720). IAS spectrum and scaled theoretical counting error contribution, using the standard DAQ system approach.

5.3.2 Using the standard DAQ system approach

The IAS spectrum obtained using the AVL encoder with the standard DAQ system approach (with correction of the geometric error) is shown in figure 9 (right) for 2 rotation speeds, up to order 360. The global shape of the spectra are identical to those obtained using the Heidenhain encoder with the high frequency counting method. The high frequency part of the spectrum has the shape of a counting error spectrum. However, the level of the counting error with the standard DAQ system approach is more difficult to predict theoretically than for the high frequency counting method. Thus, the theoretical error spectra have been scaled so as to fit the measured IAS spectra at high frequencies. The standard deviation of the detection error τ obtained experimentally from the scaling are given in table 4 for two rotation speeds. The ratio of the standard deviations to the sampling period are also given in table 4, giving a idea of the precision improvement due to the interpolation of the zero crossings of the angle encoder signal. At 52 rad/s (500rpm), the detection error standard deviation is about 500 times lower than the sampling period, which illustrate the possibility to reach a good precision with the standard DAQ system approach. At this rotation speed, the detection uncertainty is indeed only 5 times higher than the uncertainty obtained using the high frequency counting approach, while the frequency sampling is about 800 times lower (80 MHz over 102400 Hz). This remarkable result can be explained by the fact that the encoder signal is acquired with a high dynamic (24 bits) with the standard DAQ system, allowing a fine interpolation of zero crossings, while the dynamic of the encoder signal that could be reproduced from the high frequency counting method is only 1 bit, making impossible any interpolation between two samples.

Rotation speed (rad/s)	std(τ)	ratio $f_e/\text{std}(\tau)$
10.5	50e-9s	220
52	20e-9s	500

Table 4: Measured standard deviation of τ for the standard DAQ system counting method

6 Conclusion

An overview of different types of IAS measurement errors has been given in this paper: the spectral aliasing error, the counting error and the geometric error. The counting error has been theoretically studied for two counting methods, one method using a high frequency clock and a counter, and one method based on the post processing of the encoder signal recorded using a standard DAQ system. A correction of the geometrical error based on calibration measurements has been proposed. The theoretical results have been illustrated on

experiments realized on a lathe. The geometric error correction has been significantly attenuated for one of the two tested encoders. One important results concerns the counting error, that has been found to be higher experimentally than theoretically using the high frequency counting approach, particularly at low speed. The error caused by the electronic device, that is not considered in the theoretical expression of the counting error in this work, is thus certainly important to consider.

References

[1] P. Charles, J. K. Sinha, F. Gu, L. Lidstone, and A.D. Ball. Detecting the crankshaft torsional vibration of diesel engines for combustion related diagnosis. *Journal of Sound and Vibration*, 321:1171–1185, 2009.

[2] M. Desbazeille, R.B. Randall, F. Guillet, M. El Badaoui, and C. Hoisnard. Model-based diagnosis of large diesel engines based on angular speed variations of the crankshaft. *Mechanical Systems and Signal Processing*, 24(5):1529–1541, 2010. Special Issue: Operational Modal Analysis.

[3] Quentin Leclère and Nacer Hamzaoui. Using the moving synchronous average to analyze fuzzy cyclostationary signals. *Mechanical Systems and Signal Processing*, 2013. In Press, Corrected Proof, Available online.

[4] Didier Remond. Practical performances of high-speed measurement of gear transmission error or torsional vibrations with optical encoders. *Measurement Science and Technology*, 9(3):347, 1998.

[5] L. Renaudin, F. Bonnardot, O. Musy, J.B. Doray, and D. Rémond. Natural roller bearing fault detection by angular measurement of true instantaneous angular speed. *Mechanical Systems and Signal Processing*, 24(7):1998 – 2011, 2010. Special Issue: ISMA 2010.

[6] M. Lamraoui, M. Thomas, M. El Badaoui, and F. Girardin. Indicators for monitoring chatter in milling based on instantaneous angular speeds. *Mechanical Systems and Signal Processing*, 2013. In Press, Corrected Proof, Available online.

[7] X. Kong. *Gear train monitoring by transmission error method.* PhD thesis, University of Wisconsin–Madison, 1987.

[8] Yuhua Li, Fengshou Gu, Georgina Harris, Andrew Ball, Nick Bennett, and Ken Travis. The measurement of instantaneous angular speed. *Mechanical Systems and Signal Processing*, 19(4):786–805, 2005.

[9] K.R. Fyfe and E.D.S. Munck. Analysis of computed order tracking. *Mechanical Systems and Signal Processing*, 11(2):187–205, 1997.

[10] Fengshou Gu, Isa Yesilyurt, Yuhua Li, Georgina Harris, and Andrew Ball. An investigation of the effects of measurement noise in the use of instantaneous angular speed for machine diagnosis. *Mechanical Systems and Signal Processing*, 20(6):1444–1460, 2006. Special Issue: Laser Doppler Vibrometry.

[11] H. André, F. Girardin, A. Bourdon, J. Antoni, and D. Rémond. Precision of the ias monitoring system based on the elapsed time method in the spectral domain. *Mechanical Systems and Signal Processing*, 2013. In Press, Corrected Proof, Available online.

[12] Alessandro Rivola and Marco Troncossi. Zebra tape identification for the instantaneous angular speed computation and angular resampling of motorbike valve train measurements. *Mechanical Systems and Signal Processing*, 2013. In Press, Corrected Proof, Available online.

[13] Matthieu Boucaud, Céline Sandier, Nicolas Totaro, Quentin Leclere, Didier Remond, and Joël Perret-Liaudet. Improved acoustical sources location in gear power transmissions. In *Proceedings of the 18th Symposium Vibrations, Shocks and Noise*, page paper N ° 40, Clamart, France, July 2012.